ESTIMATION OF THE QUANTUM EFFICIENCY OF PHOTOSYNTHESIS. I. THEORETICAL GROUND AND EXPERIMENTAL APPROACHES

Yuzeir Zeinalov*, Liliana Maslenkova

Acad. M. Popov Institute of Plant Physiology, Acad. G. Bonchev Str., Bl. 21, 1113 Sofia, Bulgaria

Summary. All preceding investigations on the quantum efficiency of photosynthesis, starting with the early experiments of Warburg and Negelein (1922a, b) and Emerson and Lewis (1939, 1941) are performed under low irradiances, even under light compensation point, assuming that the photosynthetic "light curves" are linear and the quantum efficiency of photosynthesis is maximum under these conditions.

However, as it was shown in our investigations (Zeinalov, 1977a, b; Zeinalov and Maslenkova, 1980, 1996) "light curves" of photosynthesis are non-linear or "S"-shaped. In this work a special polarographic oxygen electrode system is described allowing irradiation with background light, and some principal problems existing in the experiments dealing with the maximum value of photosynthetic quantum efficiency are considered.

Key words: Emerson transient effect, oxygen induction phenomena, photosynthsis, quantum efficiency

Introduction

The quantum efficiency of a given photochemical process is determined as a ratio between the number of reacted molecules or the molecules of the reaction product and the number of the absorbed photons. In the case of photosynthesis quantum efficiency could be calculated as the ratio of the number (moles) of CO_2 molecules reduc-

---

* Corresponding author: E-mail: zeinalov@obzor.bio21.bas.bg

ed or O_2 molecules evolved and the number of the photons absorbed by the photosynthesising system. For the estimation of the quantum efficiency of photosynthesis we need: i) to determine the number of the photons absorbed by the photosynthesising system (plant leaves, algae or chloroplast suspension) and ii) to determine the number of CO_2 molecules reduced or O_2 evolved.

Obviously, the quantum efficiency of a given photochemical process could be defined as the tangent of the angle between the irradiance curve dependence of the process and the abscissa axis if the ordinate and abscissa axes are expressed as molecules (moles) evolved oxygen or reduced carbondioxide and number (moles) of absorbed photons per unit time, respectively. If the irradiance dependence of photosynthesis is a linear function the estimation of quantum efficiency could be done at any irradiance intensity. As about photosynthesis, in many experiments it was shown that even under very low light intensity conditions the photosynthetic "light curves" start with straight line part (Fig. 1-a). With the increase of irradiation the slope of the curves decreases until saturation plateau is reached. In a significant part of the experiments it was also shown that the shape of the light curves has a logarithmic part (Fig. 1-b) with a maximum slop (maximum quantum efficiency) at the beginning of the curves, i. e. when the irradiance is going to zero. The "S"-shaped curves, like to this shown on Fig. 1-c are obtained in limited number of investigations showing that the quan-
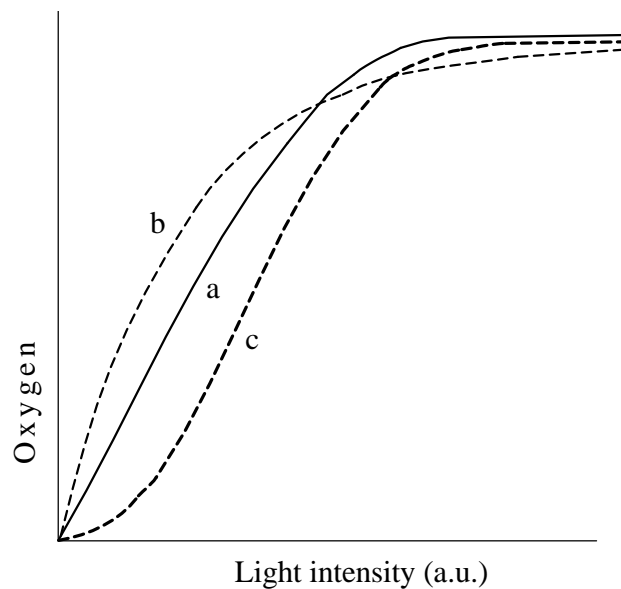

Fig. 1. Different kinds of photosynthetic "light curves". a – linear; b – logarithmic and c – "S"-shaped irradiance dependence of photosynthesis.

tum efficiency under low light intensities is tending to zero (For a review of the early investigations see E. Rabinowitch, 1951). This kind of curves obtained in green plants was interpreted by the authors in favour of an assumption about the existence of a "photic threshold" of photosynthesis. However, this view has not been accepted, and the results obtained by most authors were in support of the linear character of the light curves of photosynthesis. Lately, after the postulation of the concept of the photosynthetic unit, in 1948 Kok discovered that the initial slope of the light curves, below the light compensation point, is significantly higher and that near this point an abrupt change in the value of the quantum efficiency of photosynthesis could be observed (Kok, 1948). This observation was called "Kok's effect" and was explained with a change in the rate of dark respiration after applying irradiation.

On the other hand, in our preceding investigations (Zeinalov, 1977a, b; Zeinalov and Maslenkova, 1980, 1996) it was shown that the irradiance dependence of photosynthesis under very low irradiance conditions should be a non-linear ("S"-shaped) function. This kind of dependence is a consequence of the photosynthetic oxygen evolving mechanisms, connected with the non-cooperative (independent) action of the oxygen evolving centres, according to the model of Kok et al. (1970). It could be shown that if the centres work independently from each other, for the production of one O_2 molecule 4 electrons should be transferred, and if the obtained photoproducts are unstable in the dark, then under low irradiance conditions (when the capturing of the light quanta by the centres is realised after several seconds or even minutes), the deactivation reactions of the S_i states will lead to a decrease of the slope of the irradiance curves, i. e. to the decrease of quantum efficiency (Fig. 1-c).

All preceding investigations on quantum efficiency of photosynthesis, starting with early experiments of Warburg and Negelein (1922a, b) and Emerson and Lewis (1939, 1941) are performed under low irradiances, even under the light compensation point, assuming that the photosynthetic "light curves" are linear and the quantum efficiency of photosynthesis is maximum under these conditions.

However, if the "light curves" of photosynthesis are non-linear or they are "S"-shaped, the exact estimation of quantum efficiency requires compensation of the initial non-linear part of the light curves with background light and the calibrated monochromatic light beam, with known photon flux, should be applied after reaching the region of the middle straight part of the curves. Most likely the increase in quantum efficiency in the experiments of Vennesland (1966) by second (blue) light beam and the "enhancement effect" of Emerson (Emerson, 1957) are due to the non-linearity of the "light curves" under low irradiance conditions.

The aim of this work is to describe a special polarographic oxygen electrode system, allowing irradiation with background light, and to consider some principal problems existing in the experiments dealing with the maximum value of photosynthetic quantum efficiency.

Experimental setup

The block diagram of the used equipment is presented on Fig. 2. Two light beams obtained from two halogen lamps (100 W/15 V) (1, 1′), two collimators (2, 2′) and two interference filters (3, 3′) are directed to the polarographic cuvette (4). The role of the collimators is to produce parallel light beams, with homogeneously distributed light intensity. Two kinds of interference filters are used – 650 and 675 nm. The suspension of unicellular alga cells is stirred using a magnetic stirrer (5). The light beam 1 is the actinic (calibrated) light, photon flux density of which is used for the quantum efficiency determination. It is directed vertically to the top window of the cuvette. The light beam 1′ (background light source) is directed horizontally to the side window of the cuvette. This second light beam is used for the compensation of the initial non-linear part of the photosynthetic "light curves".
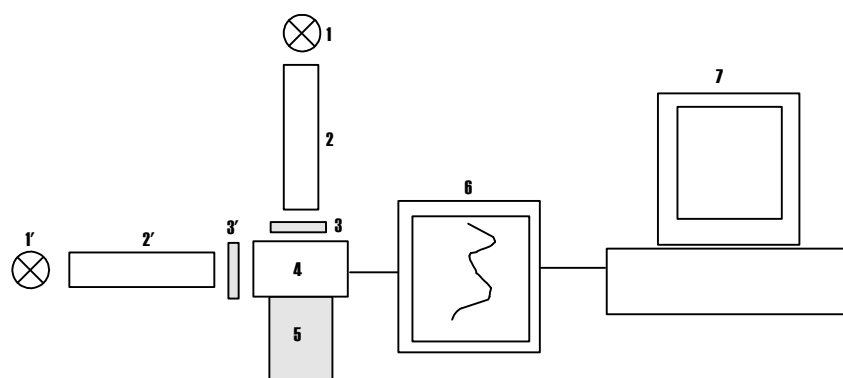

Fig. 2. Experimental set-up for quantum efficiency investigations. 1 and 1′ – halogen lamps (100 W/12 V); 2 and 2′ – collimators; 3 and 3′ – interference filters (650 nm); 4 – polarographic cuvette with oxygen electrode; 5 – magnetic stirrer; 6 – polarograph (OH-105, Radelkis, Hungary); 7 – IBM compatible computer.

The number of oxygen molecules evolved by the photosynthetic process is estimated using a polarographic oxygen electrode. The construction of the polarographic cuvette is presented on Fig. 3. The volume (approximately 20 cm^3) of the cuvette is a rectangular prism with 3×3 cm bases, fixed by two glass windows, and 2.2 cm altitude. The oxygen electrode is mounted on one of the side walls of the cuvette. The scheme and the description of the electrode is presented on Fig. 4. The oxygen electrode is easily mounted to the side wall of the cuvette after the filling of the cuvette. A small hole on the top side of the cuvette allows the excess of the suspension to lick out. The output of the polarograph (OH-101, Radelkis, Hungary) is connected to an IBM compatible computer using an AD convertor.

After applying 650 mV voltage, so that the platinum electrode is made negative with respect to the silver electrode, the sensitivity of the oxygen electrode is determin-
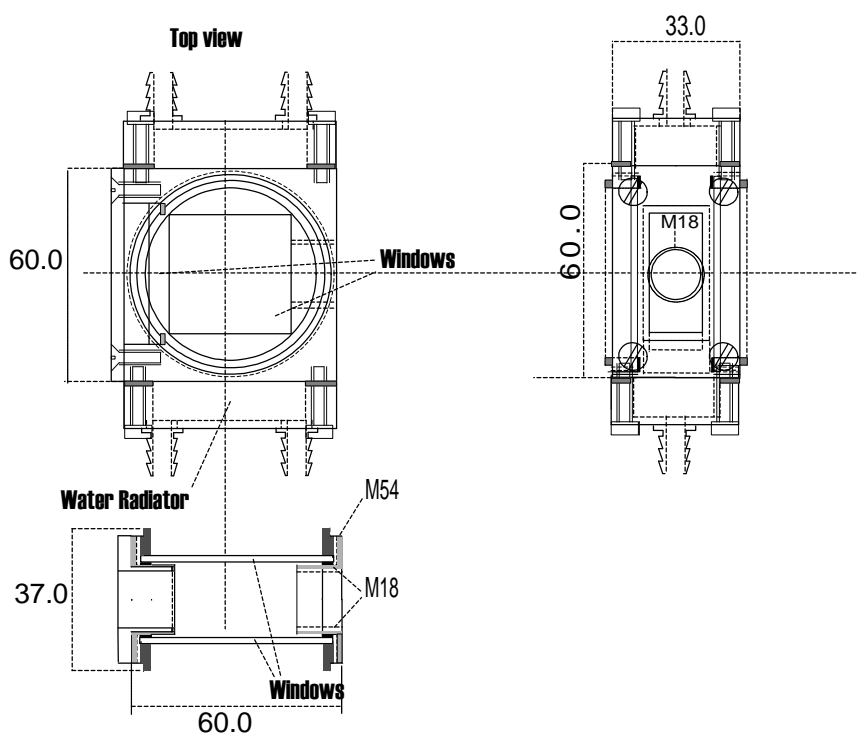
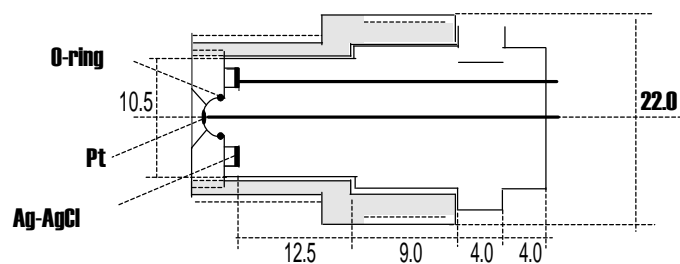**Fig. 3**. Detailed diagram of the polarographic cuvette.

Fig. 4. Polarographic oxygen electrode.

ed using distilled water in equilibrium with the air, and equal $0.276\,\mu\text{mol}\,O_2$ in 1 ml at standard conditions (760 mm Hg and 25 °C). Oxygen electrode sensitivity is calculated as:

$$k = 0.276\,\mu\text{mol}\,O_2/\Delta I.\text{ml},$$

where ΔI is the difference between the polarographic currents $(I_1 - I_2)$, (Fig. 5) obtained after using equilibrated with air water (I_1), and the same water after addition of a several crystals of dithionite $(N_2S_2O_4)$, which consumes all of the oxygen from
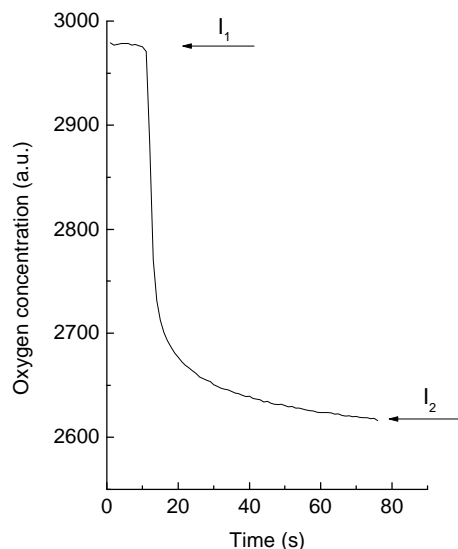
Fig. 5. The calibration record of the polarographic oxygen electrode. I_1 – polarographic current for distillated water saturated with atmospheric oxygen (0.276 µmol O_2/ml) and I_2 current after addition of the several crystals of dithionite. Polarograph sensitivity – 10^{-7} A/Div.

water (zero oxygen concentration) – (I_2). Calculation of the oxygen evolution rate could be made using the relation:

$$P = k.\,\Delta I'.V/t,$$

where $\Delta I'$ is the change in the amperometric current after illumination of the suspension for a time t (s), and V (ml) is the volume of the cuvette (suspension).

As an illustration of the equipement is presented on Fig. 6 (solid curve) changes in oxygen concentration in suspension of *Scenedesmus acutus* cells in darkness (line L1), after switching on the two light sources (the background irradiation and the calibrated light beam (I_M) – L2, after switching off the calibrated (I_M) light beam – L3, and background (I_B) irradiation – L4. Line L5 represents the increase of the oxygen concentration produced by the calibrated (I_M) light beam, L6 – after addition of the
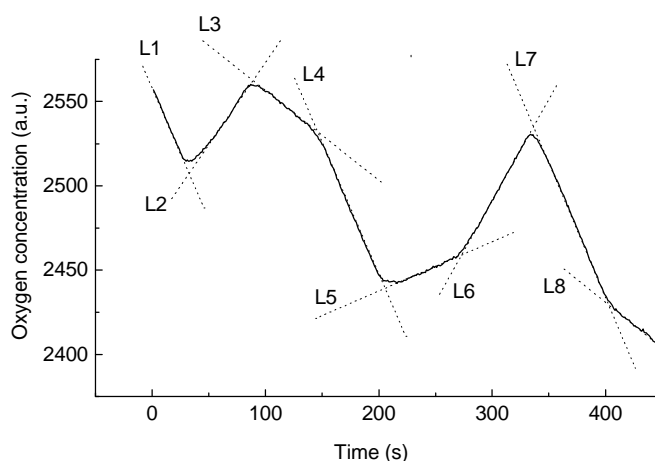

Fig. 6. Changes in the O_2 concentration in suspension of *Scenedesmus acutus* cells after irradiation with the two light beams. Lines L1, L4 and L7 – reflect the oxygen consumption connected with dark respiration of the algae cells. Lines L2 and L6 – show the increase of the O_2 concentration after irradiation with the two light beams simultaneously. L3 and L8 – the effect of switching the background (I_B) beam. L5 – the effect of the measuring (I_M) light beam.

background (I_B) irradiation, L7 – after switching off the two ($I_B + I_M$) light beams and finally L8 – after switching on the background (I_B) light beam.

The straight lines on Fig. 6 are drawn using a special programme, which allows the selection of two points (at the beginning and at end of the straigth parts on the curve) and using the procedure of linear regression are calculated the tangents of the selected straight lines. A protocol of the obtained results from the data presented on Fig. 6 is shown below:

Experiment name: Test

Date: 08/07/99

Parameters of measurements:

Number of points averaged = 10

Electrode sensitivity:

Oxygen concentration in water = 0.276 µmol O_2/ml

Polarograph sensitivity at calibration = 1.10^{-7} A/Div

Deviation for equilibrated with air and zero oxygen concentration = 63 mm

Polarograph sensitivity at measurement = 1.10^{-8} A/Div

K = $1.095.10^{-3}$ µmol O_2/Div.ml

Tangents of the lines	Oxygen evolution rates (µmol O_2/h)
Line 1 = -0.492	Line 2 - Line 1 = 15.66
Line 2 = 0.291	Line 3 - Line 2 = -9.28
Line 3 = -0.173	Line 4 - Line 3 = -6.50
Line 4 = -0.498	Line 5 - Line 4 = 11.84
Line 5 = 0.094	Line 6 - Line 5 = 5.70
Line 6 = 0.379	Line 7 - Line 6 = -17.46
Line 7 = -0.494	Line 8 - Line 7 = 6.66
Line 8 = -0.161	

Where the tangents of lines 1, 4 and 7, respectively -0.492, -0.498 and -0.494 reflect the rate of cells dark respiration. And:

A. Line 2 - Line 1 = 15.66 µmol O_2/h, is the O_2 evolution rate produced by the two light beams;

B. Line 3 - Line 2 = -9.28 µmol O_2/h, is the O_2 evolution decrease after switching off the calibrated light beam;

C. Line 4 - Line 3 = -6.50 µmol O_2/h, is the O_2 evolution decrease after switching off the background light beam;

D. Line 5 - Line 4 = 11.84 µmol O_2/h, is the O_2 evolution rate produced by the calibrated light beam (as B);

E. Line 6 - Line 5 = 5.70 µmol O_2/h, is the O_2 evolution rate produced by the background light beam (as C);

F. Line 7 - Line 6 = -17.46 µmol O_2/h, is the O_2 evolution decrease after switching off both light beams (as A);

G. Line 8 - Line 7 = 6.66 µmol O_2/h, is the O_2 evolution rate produced by the background light beam (as C and E);

Considering the obtained results it could be said that the value of dark respirations remains almost constant while the variation in the values of photosynthetic oxygen evolution rate exists and an explanation of these deviations will be given in the last part of the paper where the induction and transient effects are considered.

The determination of the absorbed photon number

The energy distribution of the electromagnetic spectrum of the halogen lamp between 400 and 750 nm, using the Spectroradiometer "MACAM" model SR3000A is presented on Fig. 7. The number of photons at the monochromatic light beam, obtained by the 650 nm (Fig. 8) interference filter, is estimated after determination of the energy of the photon flux. The photon flux density is calculated according to the expression:

$$n_{h\nu}(mol) = E_0 \, (W.cm^{-2})/E_m \, (J.mol^{-1}),$$

where E_0 is the integrated energy distribution after the interference filter in $J.cm^{-2}.s^{-1}$ and E_m is the energy of 1 mol photons at the same wavelength ($18.4.10^4 \, J.mol^{-1}$ for the 650 nm light beam).

The construction of the polarographic cuvette allows the determination of the transmitted (E_t) as well as the reflected part (E_r) of the irradiance energy. The reflected
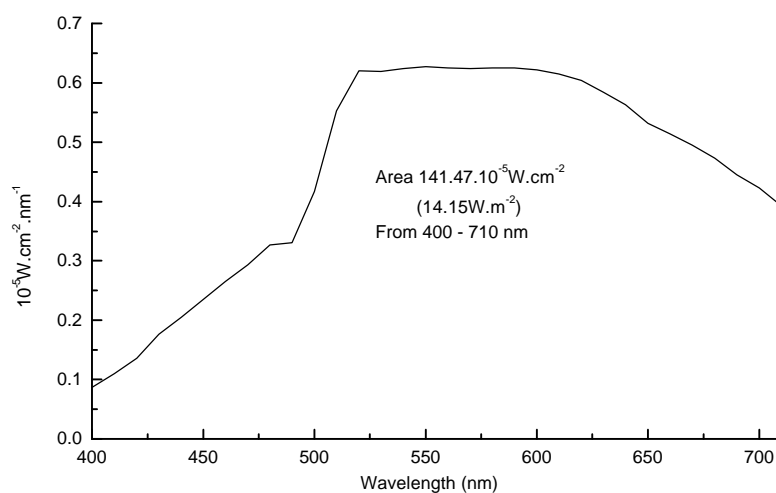
Fig. 7. Spectral distribution of the irradiance energy at halogen lamp – 100 W/12 V.
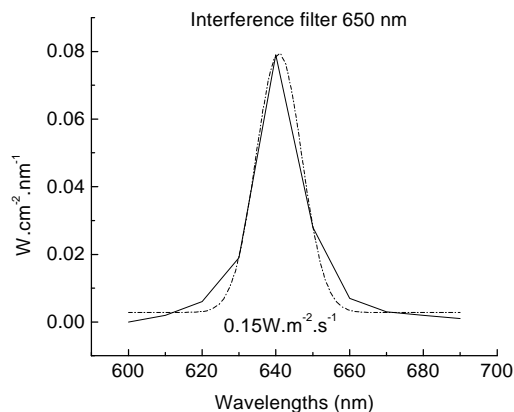
Fig. 8. Spectral distribution of the energy after the 650 nm interference filter (solid line) and a Gauss function approximation (dashed line).

from the top surface of suspension (top window) total irradiance energy (E_r) is determined using the spectrophotometer SF4 (USSR) equipped with an Ulbricht sphere and this of the transmitted part (E_t) is determined by the help of calibrated selenium photosensor. Then the number of the absorbed quanta for a second could be obtained using the relation:

$$n'_{h\nu} \, (mol) = n_{hn}(mol).(E_0 - E_r - E_t)/E_0.$$

The second way to estimate the number of absorbed photons is the determination of the energy of the transmitted light beam with the cuvette filled with nutrition solution E'_0 and the energy of the same light beam (E'_t) with cuvette filled with algae or chloroplast suspension. Then the number of absorbed light quanta could be calculated using the relation:

$$n'_{h\nu}(mol) = (E'_0 - E'_t)/E_m.$$

Interference of induction and transient phenomena

The investigations of the living systems are connected with some specific problems as they are continuously changing systems and simultaneously they are in possession of highly developed memory, which allows them to keep in mind for a long time all preceding living history. So, the investigations of quantum efficiency using unicellular algae should be done having in mind that the suspension optical density, i. e. the irradiance absorption property is a variable parameter as the number of the cells and their dimensions during the experiment time are not constants. This imposes the optical parameters (E_t, E_r, E'_0 and E'_t) of the suspensions and the polarographic cuvette

to be measured before, during and after the experimental procedure connected with estimation of the functional parameters.

A special problem represents the so-called induction and transient effects. The establishment of a new steady state level after an abrupt change of conditions (illumination, temperature, etc.) in the complex photosynthetic photophysical and photochemical events is connected to some specific transitory phenomena.

Oxygen and fluorescence transitory phenomena became familiar as early as 1931, when Kautsky and Hirsh reported about specific and highly reproducible fluorescence emission intensity changes after light excitation. In 1939 Emerson and Lewis observed changes in the photosynthetic O_2 and CO_2 exchange following the light-dark and dark-light transients. A considerable number of papers related to the subject followed. Nevertheless, many questions about the nature of the induction phenomena are still open.
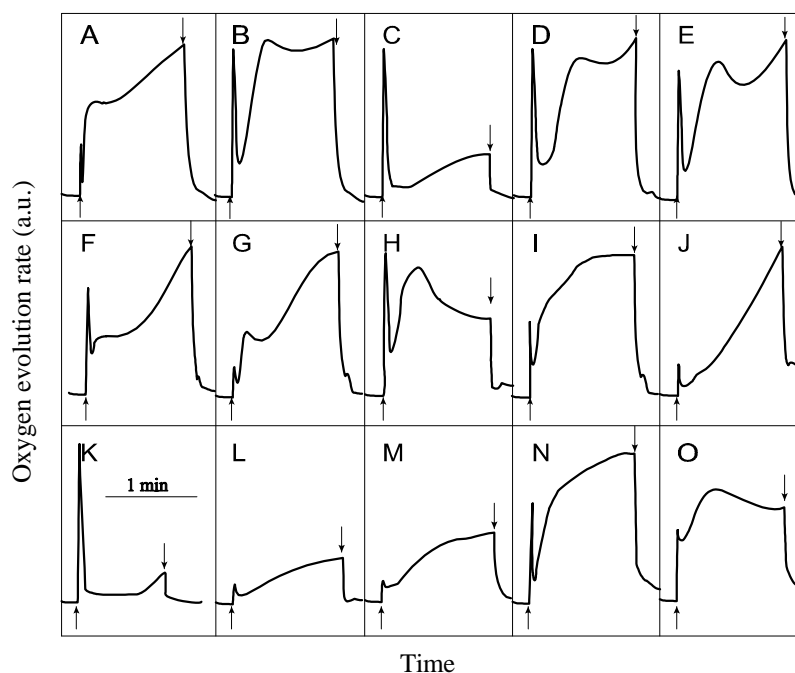

Fig. 9. Oxygen induction curves in different species and strains of *Scenedesmus* and *Chlorella*. Light period 30 s. Dark incubation time 4 min. A – *Chl. vulgaris*, 3.10^{-7} A/mm; B – *Chl. vulgaris*, 6.10^{-8} A/mm; C – *Chl. vulgaris*; 6.10^{-8} A/mm; D – *Chl. vulgaris*, 8.10^{-8} A/mm; E – *Chl. vulgaris*, 4.10^{-8} A/mm; F – *Sc. acutus*, strain Ilkov 71/10, 1.10^{-7} A/mm; G – *Sc. obliquus*, strain Lhotsky 1966/7, 2.10^{-7} A/mm; H – *Sc. obliquus* strain Lhotsky 1966/7, 8.10^{-8} A/mm; I – *Sc. obliquus* strain Lhotsky 1966/7, 1.10^{-7} A/mm; J – *Sc. acutus*, strain Tomaselli 8, 2.10^{-7} A/mm; K – *Sc. abondans*, strain Ilkov 15/73, 6.10^{-9} A/mm; L – *Sc. obliquus*, strain 13 (Leningrad), 8.10^{-9} A/mm; M – *Sc.* sp., strain Ilkov 10-2/72, 6.10^{-8} A/mm; N – *Sc. obliquus*, strain Lhotsky 1966/7, 6.10^{-8} A/mm; O – *Sc. acutus*, strain Ilkov 17/72, 3.10^{-7} A/mm.

The significant variety of oxygen induction curves observed in different species and strains of green unicellular algae are shown on Fig. 9. They have been registered using a polarographic oxygen rate electrode, analogous to the electrode of Joliot and Joliot (1968). An initial oxygen burst is present in all samples. In a considerable number of curves it is followed by a distinct minimum and gradual transition to steady state level with an obvious slowing down in the increase of oxygen evolution rate that is expressed as a second minimum. Presumably, the differences observed among the curves were due not only to certain features characteristic for every species, but are determined considerably by the different physiological state of algae studied. No doubt, one and the same environmental conditions (temperature, light, CO_2 concentration, etc.) could be optimal or close to optimal for some of the species and far of optimal for the others. Thus, the standardisation of algae growth conditions and oxygen evolution does not mean equal conditions (in the sense of equal optimisation) for all algae species and strains. It must be noted that oxygen induction curves, shown in Fig. 9, were selected from a great number of experimental curves with the aim to show the differences in their character. The data obtained show that induced oxygen evolution was accompanied by complex kinetic transitions.
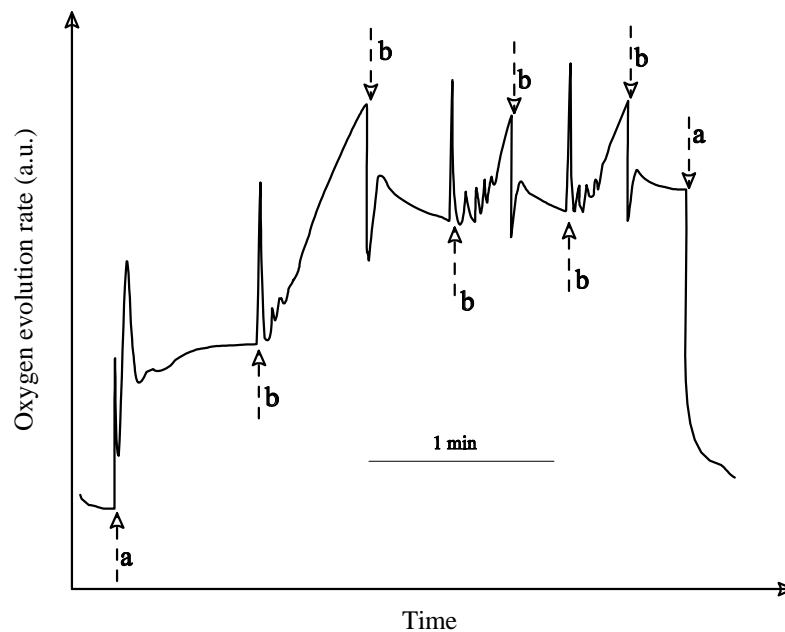

Fig. 10. Emerson transient effect in *Chlorella pyrenoidosa*. Two light beams are used: a – 30 000 W/m² and b – 100 000 W/m². The consecutive switching on and off of the light beam b produced the appearance of the transient effect with well expressed oscillations in the oxygen evolution rate.

Another type of transient effects are the so-called "Emerson transients" arising every time when the irradiation is submitted to an abrupt change. The results presented on Fig. 10 illustrate this kind of transients, obtained with a suspension of *Chlorella pyrenoidosa* irradiated with two different light beams. It is evident that after the switching off and on of the second light beam "b" the establishment of a new steady state level is reached after several seconds (minutes).

The presented results show that the investigations of the action spectra or quantum efficiency spectra and the maximum value of the quantum efficiency of photosynthesis is significantly complicated by the non-linearity of the irradiance curves and by the existing transient effects. The oxygen induction phenomena presented on the last two figures explain the variation in the oxygen evolution rate presented on Fig. 6. It could be seen that at the beginning of the experiments (Line 2 – Line 1) the effect of the two light beams ($I_B + I_M$) on this figure is 15.66 µmol O_2/h, while in the end (Line 7 – Line 6) this value is 17.46 µmol O_2/h. Analogous variations could be seen for the effect of the separated light beams.

References

Emerson, R., C. M. Lewis, 1939. Factors influencing the efficiency of photosynthesis. Am. J. Botany, 26, 808–822.

Emerson, R., C. M. Lewis, 1941. The quantum efficiency of photosynthesis. Carnegie Inst. Yearbook, 40, 157–160.

Emerson, R., 1957. Dependence of yield of photosynthesis in long-wave red on wavelength and intensity of supplementary light. Science, 125, 746.

Joliot, P., A. Joliot, 1968. A Polarographic method for detection of oxygen production and reduction of Hill reagent by isolated chloroplasts. Biochim. Biophys. Acta, 153, 625–634.

Kautsky, H., A. Hirsh, 1931. Neue Versuche zur Kohlenstoffassimilation. Naturwissenschaften, 19, 964–968.

Kok, B., B. Forbush, M. McGloin, 1970. Co-operation of charges in photosynthetic O_2 evolution. I. A linear four step mechanism. Photochem. Photobiol., 11, 457–475.

Kok, B., 1948. A critical consideration of the quantum yield of *Chlorella* - photosynthesis. Enzymologia, 13, 1–56.

Rabinowitch, E. I., 1951. Photosynthesis and Related Processes, Vol. II, Interscience Publichers, New York.

Vennesland, B., 1966. The energy conversion reactions of photosynthesis. In: Biochemical Dimensions of Photosynthesis. Eds. D. W. Krogmann and W. H. Powers, pp. 48–61.

Warburg, O., E. Negelein, 1922a. Ueber den Energieumsatz bei der Kohlensaeureassimilation. Zeitschr. F. Phys. Chem., 102, 235–266.

Warburg, O., E. Negelein, 1922b. Ueber den Einfluss der Wellenlaenge auf den Energieumsatz bei der Kohlensaeureassimilation. Zeitschr. F. Phys. Chem., 106, 191–218.

Zeinalov, Y., L. Maslenkova, 1996. Mechanisms of photosynthetic oxygen evolution. In: Handbook of Photosynthesis, Ed. M. Pessarakli, Marsel Dekker, Inc., N.Y., pp. 129–150.

Zeinalov, Y., L. Maslenkova, 1980. Analysis of action spectra of photosynthesis. Photosynthetica, 14(4), 512–516.

Zeinalov, Y., L. Maslenkova, 1980. Red drop of quantum efficiency and Emerson's second effect as direct consequences of the principle of non-additive action of light in photosynthesis. Photosynthetica, 14(4), 506–511.

Zeinalov, Y., 1977a. Non-additivness in the action of light at the photosynthesis of green plants. Copmt. rend. Acad. bulg. Sci., 30(10), 1479–1482.

Zeinalov, Y., 1977b. The principle of non-additivness in the action of light and the concept of two photosystems at the photosynthesis in green plants. Copmt. rend. Acad. bulg. Sci., 30(11), 1641–1644.